Multi-beam effects on backscatter and its saturation in experiments with conditions relevant to ignition[a)]

R. K. Kirkwood,[1,b)] P. Michel,[1] R. London,[1] J. D. Moody,[1] E. Dewald,[1] L. Yin,[2] J. Kline,[2] D. Hinkel,[1] D. Callahan,[1] N. Meezan,[1] E. Williams,[1] L. Divol,[1] B. L. Albright,[2] K. J. Bowers,[2] E. Bond,[1] H. Rose,[2] Y. Ping,[3] T. L. Wang,[4] C. Joshi,[4] W. Seka,[5] N. J. Fisch,[6] D. Turnbull, [6]S. Suckewer,[6] J. S. Wurtele,[7] S. Glenzer,[1] L. Suter,[1] C. Haynam,[1] O. Landen,[1] and B. J. Macgowan[1]
[1]*Lawrence Livermore National Laboratory, Livermore, California 94551, USA*
[2]*Los Alamos National Laboratory, Los Alamos, New Mexico 87545, USA*
[3]*Institute of Laser Sciences and Applications, Lawrence Livermore National Laboratory, Livermore, California 94551, USA*
[4]*Department of Electrical Engineering, University of California at Los Angeles, Los Angeles, California 90095, USA*
[5]*University of Rochester - Laboratory for Laser Energetics, Rochester, New York 14623-1299, USA*
[6]*Department of Astrophysical Sciences, Princeton University, Princeton, New Jersey 08544, USA*
[7]*Department of Physics, University of California at Berkeley, Berkeley, California 94720, USA*

(Received 20 November 2010; accepted 29 March 2011; published online 26 May 2011)

To optimize the coupling to indirect drive targets in the National Ignition Campaign (NIC) at the National Ignition Facility [E. Moses *et al.*, Phys. Plasmas **16**, 041006 (2009)], a model of stimulated scattering produced by multiple laser beams is used. The model has shown that scatter of the 351 nm beams can be significantly enhanced over single beam predictions in ignition relevant targets by the interaction of the multiple crossing beams with a millimeter scale length, 2.5 keV, $0.02-0.05\times$ critical density, plasma. The model uses a suite of simulation capabilities and its key aspects are benchmarked with experiments at smaller laser facilities. The model has also influenced the design of the initial targets used for NIC by showing that both the stimulated Brillouin scattering (SBS) and stimulated Raman scattering (SRS) can be reduced by the reduction of the plasma density in the beam intersection volume that is caused by an increase in the diameter of the laser entrance hole (LEH). In this model, a linear wave response leads to a small gain exponent produced by each crossing quad of beams ($<\sim 1$ per quad) which amplifies the scattering that originates in the target interior where the individual beams are separated and crosses many or all other beams near the LEH as it exits the target. As a result all 23 crossing quads of beams produce a total gain exponent of several or greater for seeds of light with wavelengths in the range that is expected for scattering from the interior (480 to 580 nm for SRS). This means that in the absence of wave saturation, the overall multi-beam scatter will be significantly larger than the expectations for single beams. The potential for non-linear saturation of the Langmuir waves amplifying SRS light is also analyzed with a two dimensional, vectorized, particle in cell code (2D VPIC) that is benchmarked by amplification experiments in a plasma with normalized parameters similar to ignition targets. The physics of cumulative scattering by multiple crossing beams that simultaneously amplify the same SBS light wave is further demonstrated in experiments that benchmark the linear models for the ion waves amplifying SBS. The expectation from this model and its experimental benchmarks is shown to be consistent with observations of stimulated Raman scatter in the first series of energetic experiments with ignition targets, confirming the importance of the multi-beam scattering model for optimizing coupling. © *2011 American Institute of Physics*. [doi:10.1063/1.3587122]

I. INTRODUCTION

To successfully implode fusion capsules via the indirect drive approach, multiple laser beams must be efficiently transported to the interior of a hohlraum cavity,[1] transiting a plasma where each can potentially influence the scattering of the others. It has long been known that individual laser beams can stimulate scattering in the plasma[2] by driving waves that are frequency and wavenumber matched to scatter light back out of the hohlraum. The first demonstrations of small but significant stimulated scattering by a single beam with its intensity, and polarization profiles smoothed by a phase plate, and finite laser bandwidth, propagating in plasmas with conditions similar to ignition targets,[3–6] provided an experimental basis for the construction of the National Ignition Facility (NIF).[7] The NIF is now routinely operating with ≥ 1.3 MJ of 351 nm light in 192 beams with shaped power waveforms, incident in cones with four different angles on targets designed to produce fusion ignition by

[a)]Paper BI2 3, Bull. Am. Phys. Soc. **55**, 21 (2010).
[b)]Invited speaker.

indirect drive. The construction of NIF and the need for accurate modeling of coupling to the targets, motivated extensive experimentally benchmarked modeling of the scattering of individual beams[8,9] because of its potential to limit the coupling of energy to the ignition targets.

Shortly after the initial demonstrations of single beam scattering under these conditions, multi-beam effects that can occur when the beams intersect at large crossing angles were also predicted and demonstrated. These demonstrations included the seeding of forward stimulated Brillouin scattering (SBS) of one beam by additional beams with resonant wavelengths,[10,11] and the amplification and subsequent saturation of long wavelength light[12] can occur when single beam Raman scatter encounters additional intersecting beams. The first of these multi-beam processes was identified as being important for controlling radiation symmetry in hohlraum targets both because the high amplitude seed consisting of one or more co-propagating beams could cause significant power and energy transfer from other beams even when the overall gain exponents were <1, and because the plasma conditions in the beam crossing volume in ignition targets have the sonic flows needed to match the SBS amplification resonance when the beams have the same wavelength.[13] The demonstration of a strong wavelength dependence of seeded SBS forward scatter, or power transfer between crossing beams as it is now called, led to the concept of wavelength tuning of beams that enter ignition target at different angles[13] in order to control forward scatter and produce the laser power deposition profile needed on the interior of the hohlraum wall for symmetric implosions. As a result NIF now has wavelength tuning capability,[14] and an analysis of the SBS amplification of the forward going power of all entering beams by all other beams has been implemented and used to estimate the optimal wavelengths for the beams to produce symmetric x-ray drive in all ignition target designs. This analysis has also shown that frequency tuning can even correct the power deposition profile to compensate for other effects that distort the x-ray drive in the target.[15] Most recently, the effectiveness of ion wave power transfer between crossing beams for controlling the implosion symmetry was clearly demonstrated in initial experiments in ignition hohlraums where the measured capsule symmetry was shown to be strongly affected by changing the wavelengths of the beams from the predicted optimal values.[16] This is consistent with the occurrence of resonant amplification of beams by ion wave scattering, and allows a final empirical tune of the symmetry by variation of the wavelength.[16] These results have firmly established multi-beam laser plasma interactions as controlling the direction of energy and power flow in hohlraums. In this paper we describe how many of the concepts developed to control the forward laser power flow are also important for understanding and controlling back scattered light in these same targets.

Another early demonstration of light amplification under conditions similar to ignition targets, which is relevant to enhancement of the backscatter in National Ignition Campaign (NIC) experiments, was done with Raman scatter. Experiments showed that it is possible to transfer energy from a crossing pump beam via resonant seeded stimulated Raman scattering (SRS) when the light is near counter-propagating with the pump beams and its frequency down shift is large.[12] These measurements were the first to show that Raman scatter in ignition targets could be affected by multi-beam interactions. They also found that the power transferred was well below the predictions for scattering by linear Langmuir waves, and its scaling with beam intensity was consistent with strong wave saturation in the case studied. The saturation of SRS produced by either single or multiple beams in these conditions was difficult to model.[17,18] The difficulties arose in part because saturation could be caused not only by electron kinetic effects, such as particle trapping, but also by ion wave non-linearities such as secondary decays of the Langmuir wave into ion waves and additional Langmuir waves via the Langmuir decay instability (LDI). In fact a separate line of experiments demonstrated that SRS from a single intense beam was controlled by decreasing the damping rate of ion acoustic waves in the plasma by the removal of low Z impurities. This suggested that secondary ion wave decays controlled the level of saturation in some cases when the product of the wave number and Debye length ($k\lambda_D$) was of order 0.4.[19,20] The simulations[17,18] and subsequent measurements of wave decay products with Thomson scattering, both detected the secondary ion wave decays of SRS Langmuir waves[21–23] and showed that the ion wave decays were only significant when the $k\lambda_D$ product was low ($<\sim 0.4$).[22,23] As a result it was concluded that the higher values of $k\lambda_D$ expected in the beam crossing volume of ignition targets would prevent ion wave growth and allow only electron kinetic effects to potentially saturate SRS.

In this paper we describe the most recent models of the electron kinetic effects relevant to growth and saturation of multi-beam scatter in the range of plasma conditions of ignition targets. For example, our target design for 1 MJ of incident energy discussed below, this means the electron densities are in the range of ~ 0.02 to ~ 0.15 of critical density and electron temperatures in the range of ~ 1 keV to ~ 3 keV at different times and locations in the target. We also describe experiments on multi-beam SRS at small laser facilities that use short duration seeds to avoid the unnecessary complexity of ion wave decays of Langmuir waves in the low $k\lambda_D$ conditions that are accessible at those facilities. We further show how the experiments have benchmarked a vectorized, particle in cell code (VPIC) that models the electron kinetic effects occurring in ignition experiments. Next, we describe experiments on SBS amplification of light by multiple crossing pump beams in ignition relevant plasmas that benchmark the NIC models for the case of many crossing beams. Finally we will use these models and measurements of scatter in the NIC hohlraum targets to demonstrate the ways in which these effects are influencing the on-going ignition campaign experiments and guiding the interpretation of their results.

II. MEASUREMENT OF RAMAN AMPLIFICATION AND SATURATION WITH THE JUPITER LASER

In this section the most recent studies of SRS amplification of light by crossing pump beams in plasma conditions

TABLE I. Comparison of the plasma conditions from experiments on Raman amplification by crossing beams in plasmas, with the conditions expected in the beam crossing volumes at early and late time in the pulses in NIC experiments. In this work the effects of multiple pump beams in the NIC targets at early time are compared with VPIC simulations benchmarked by the experiments at smaller lasers. Analysis of the effects of more than one pump in NIC targets at late time is also discussed in Ref. 42.

Laser facility (yr)	$n/n_{crit.}$	$k\lambda_{Debye}$
Nova (1998)	0.07	0.40
Jupiter, LLNL (2005–2008)	0.01	0.38
NIF (early in pulse, 2009–2010)	0.03	0.68
NIF (late in pulse, 2009–2010)	0.12	0.30

similar to the NIC ignition studies are reviewed.[24–26] Those experiments are then modeled with both linear wave analysis and our massively parallel VPIC simulations[27,28] that include the electron kinetic non-linearities such as particle trapping, wave front bowing, wave mode frequency detuning, and other trapped electron effects. In Raman amplification experiments carried out at laser facilities that have much less power and energy than is needed for ignition, it has been challenging to emulate the plasma conditions where re-amplification occurs in ignition targets because the electron temperatures are very high in ignition targets (2–4 keV) so that the $k\lambda_D$ products tend to be in the range 0.4 to 0.9 which causes strong linear damping of plasma waves. As a result the intensity of the pump beam, the distance over which it interacts with the seed, and the plasma conditions needed to create the significant SRS amplification with 351 nm beams in ignition targets are hard to emulate with low energy lasers. The first demonstration of SRS amplification was carried out at the Nova laser where $k\lambda_D = 0.4$ and $n/n_{crit} = 0.07$ was achieved. More recent studies have taken advantage of lower energy beams of 1054 nm light to increase the ponderomotive force and create measureable spatial growth rates with reduced normalized plasma density n/n_{crit} and values of both $k\lambda_D$ and plasma scale lengths that are as close as possible to the ignition values. This approach has allowed experiments with the Jupiter laser to demonstrate SRS amplification while achieving $k\lambda_D = 0.4$ and $n/n_{crit} = 0.01$, which are both appropriate in different regions of the beam crossing volume in ignition experiments.[24] However, higher values of $k\lambda_D$ are expected in some parts of the SRS amplification regions in ignition experiments and will influence the saturation mechanisms there, yet have not been experimentally accessible at Jupiter, because at the low plasma densities the SRS gain becomes unmeasureably low.[24] A summary of the dimensionless plasma parameters in the small scale experiments performed to date and in the beam crossing region of the NIC ignition targets is provided in Table I.

The approach to understanding the range of ignition conditions is first to carry out experiments with short pulse seeds to determine the electron saturation on time scales too fast for ion acoustic decays to occur under the normalized plasma conditions that are as close as possible to those in the ignition target (in particular at the highest $k\lambda_D$ available). Next, VPIC simulations are performed of the electron kinetic saturation mechanisms known to be important for the still

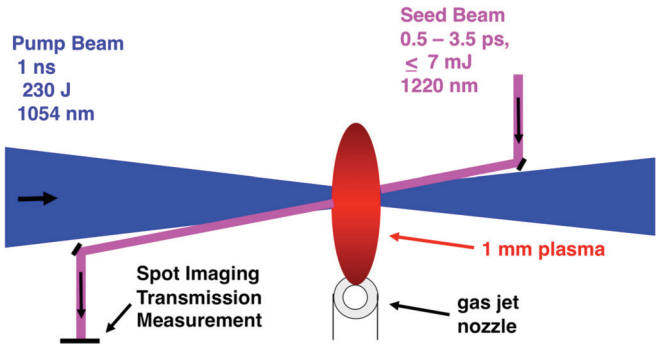

FIG. 1. (Color) Geometry of the experiments on SRS amplification by a single pump at Jupiter laser, where a >1 mm resonance region was created with normalized plasma conditions similar to the ignition targets and amplification rates were measured to bench mark models of multi-beam scattering that were used to design the ignition targets.

higher $k\lambda_D$ regions of the ignition targets and are benchmarked with the experiments. Then the benchmarked code is used to predict plasma scattering in ignition targets. The most complete studies to date were carried out at Jupiter, where the amplification of both 0.5 and 3.5 ps duration seeds of broad spectrum light by interaction with a single crossing pump beam in a strongly damped plasma ($k\lambda_D = 0.38$) with a small amplitude gain exponent (~2) was demonstrated on a time scale that does not allow ion wave instabilities. This demonstrated, for the first time under such conditions,[25,26] a non-linear, electron kinetic saturation of the amplification that has now been described by 2D VPIC simulations.[26–28] The shortest pulse used would allow the ion waves involved in secondary decays to undergo no more than 1 radian of oscillation ($wt_{pulse} \sim 1$) so they are unable to saturate the SRS Langmuir waves, which can then grow and be saturated by the electron kinetic effects relevant to the higher $k\lambda_D$ of ignition targets. Beam propagation through the crossing volume in ignition targets may, however, also be affected by enhanced beam spray and turbulence associated with a larger number of crossing pumps. The short pulse also makes these experiments and the simulations that describe them, useful for the design of plasma amplifiers and pulse compressors for ultra short pulses.[29]

The experiments were performed at the Jupiter laser facility with a 230 J, 1054 nm pump beam with a 1 ns pulse length, and a <~6 mJ, @ 3.5 ps, seed beam incident on a gas jet target. The f/10 pump beam had a focal spot of 500 micron FWHM diameter, smoothed with a phase plate and was intersected by the f/25 seed beam propagating 11° away from counter-propagating. The best focus of the seed was placed ~12 mm after the point of intersection with the pump, so that the two beams had approximately equal spot sizes in the intersection region as shown schematically in Figure 1. The beams intersected for a distance of 3 mm along either direction of propagation. A He gas jet was used as described in Refs. 24 and 30 and produced a gas profile with a flat top region of ~1.5 mm. Simulations with the Hydra code[31] of the beam incident on an initially uniform gas show a uniform plasma that forms across the profile of the spot, with the electron temperature reaching a peak value of 244 eV near the end of 1 ns pulse. The 2D Hydra

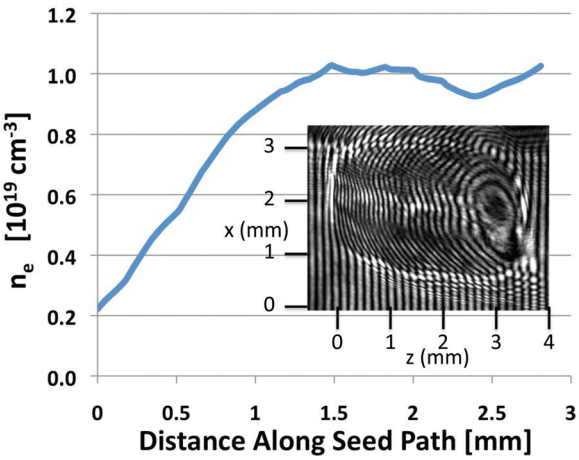

FIG. 2. (Color) The plasma density profile produced in the Jupiter experiments with gas jet targets was measured with a 2D 527 nm interferometer and verified to have the needed uniformity. The inset shows the interferometer image which is interpreted to produce the plot of the density profile along the path of the incident seed beam as discussed in the text.

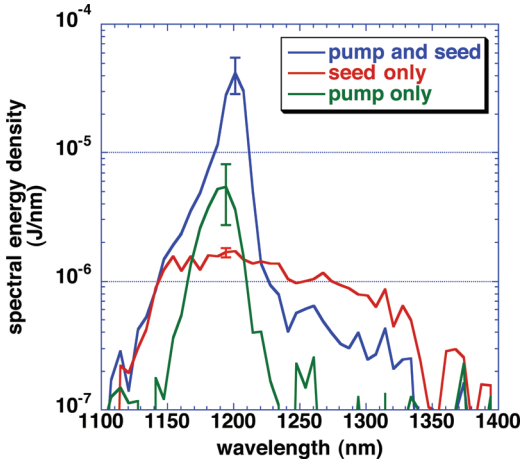

FIG. 3. (Color) The incident ("seed only") and transmitted ("pump and seed") seed spectrum observed in Jupiter experiments with a low power seed pulse having a 0.5 ps duration are shown along with the spectra produced by the scattering of the pump beam alone ("pump only"), and demonstrate substantial amplification of the transmitted light.

simulations also show that the axial profile of the density is sufficiently uniform ($dn/n <\sim 5\%$) to keep the two beams well within the half width of the peak of the resonance with the Langmuir waves, over the $<\sim 1.5$ mm of the plateau region of the gas jet and for the duration of the 1 ns pump pulse. To achieve these conditions in the experiments the gas pressure of the jet was adjusted to maximize the observed seed amplification near 1220 nm, as is consistent with the peak electron density in the interaction volume being 1.2×10^{19} cm^{-3}. The resonant region of the profile was confirmed with 2D interferometric images produced by a 527 nm beam of light that was synchronized with the seed beam and transits the plasma normal to the pump and in the same plane as the probe. The transmitted 527 nm beam is then directed normal to a 2D Charge Coupled Device (CCD) array where it is interfered with a separate beam that does not transit the plasma and is incident at a small angle to produce a series of vertical fringes in regions of the image where there is no plasma density. The plasma density present near the center of the image produces shifts in the phase of the light in that leg, leading to a shift in the position of the fringes as shown in an example in the inset of Figure 2. The density produced along the axis of the probe beam is then determined by a best fit inversion of the measured phase shift vs. position and assuming the plasma density is axi-symmetric about the pump beam. The results show that the density, and hence Langmuir wave frequency, varies by less than the half the resonance width in a region of 1 to 1.5 mm along the seed path as shown in the plot in Figure 2. To study the effect of this resonant region on the seed beam the transmitted light of the seed is both spectrally resolved and spatially imaged on a 1D CCD array at the plane of the pump beams best focus as described in Ref. 26. The energy and spot size for these experiments were chosen to maximize the beam intensity and interaction length without significantly driving filamentation in the plasma. The optimum intensity determined the results from a series of earlier experiments that observed a sharp onset of angular beam spray and scattering of the transmitted light outside the f/cone of the incident beam when intensity was in excess of the value 1.2×10^{14} W/cm^2 that is studied here.[25]

Figures 3 and 4 show the measured transmitted seed spectrum from experiments in which a 0.5 ps seed with a spectral energy density of ~ 1.5 μJ/nm near 1200 nm was intersected with the pump beam, and compares it with measurements with the seed beam only (no plasma) and the pump beam only (with plasma), at the same intensities and conditions. The data in Figure 3 clearly show the plasma amplifier both enhances and narrows the seed spectrum relative to the "seed only" case, which is consistent with Raman amplification in the uniform plasma region. The spectrum of unseeded SRS from a "pump only" experiment at the same pump intensity is also shown in the figure which demonstrates that the energy produced by un-seeded SRS is much less than the output seed energy and does not contribute

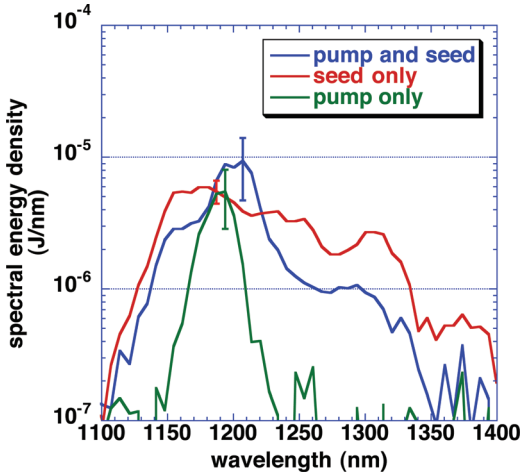

FIG. 4. (Color) The incident ("seed only") and transmitted ("pump and seed") seed spectrum and "pump only" scattering spectrum for the case of Figure 3 but with increased seed power, showing a dramatic reduction in transmission and amplification with increased power.

significantly to the observed amplification. When the spectrally integrated transmitted energy was spatially resolved near the focus, similar enhancements were observed as discussed in Ref. 26. The observed amplification is not found to depend strongly on the timing for the seed between 200 and 900 ps in these experiments consistent with the simulated slow evolution of plasma conditions. Inverse bremsstrahlung absorption in the plateau region of the plasma is <5% of the incident energy and does not significantly affect the amplification factor.

A second experiment carried out under the same conditions but with the incident seed intensity increased to ~5 μJ/nm near 1200 nm is shown in Figure 4 with the associated seed only and pump only measurements. This data demonstrates that the observed peak spectral amplification ratio between the incident and transmitted seed significantly reduces as the seed intensity is increased. This is consistent with the Langmuir waves involved in the amplification being saturated so that their amplitude and the power they scatter from the pump do not increase linearly with the incident seed intensity. In fact in this case the transmitted spectral intensity is reduced relative to the case of Figure 3 because the seed intensity is increased, suggesting a very strong Langmuir wave saturation is occurring.

To further study the response of the Langmuir waves responsible for the amplification of light on this time scale, a series of experiments were performed both with 3.5 and 0.5 ps seeds with the input seed power varying from 8×10^6 to 2×10^9 W. The amplification factor was calculated from the measured spectral and spot profiles as described in Refs. 25 and 26. The spectral amplification was determined to be as high as 77× for the 3.5 ps seed with an incident power of 8×10^6 W and greatly reduced or absent for incident powers ranging from 4.5×10^8 to 1.6×10^9, The amplification factor was also measured from the spot profile data and was found to track the spectral amplification factor in the cases studied. If the waves were responding linearly to the ponderomotive force, the amplification factor would be expected to be independent of the seed power.[2] However, the data clearly shows the amplification factor to be non-linearly reduced, or saturated, at seed powers $>1 \times 10^8$ W, becoming negligible at 4.5×10^8 W, and either fluctuating or slightly increasing at the highest powers studied as shown in Figure 5. This demonstrates non-linear saturation of the wave response and/or reduced coherence of the fields at high seed intensity. Moreover, we estimate the linear SRS gain rate for the simulated experimental conditions and a 1.2 mm interaction length as shown by the line in Figure 5, and find that the observed amplifications, especially at the highest seed intensity, are well below this value, which is also consistent with non-linear effects reducing the wave response and scatter when the seed is large. The maximum transmitted energy in the 3.5 ps seed in these cases is $<\sim 14$ mJ, and the associated energy deposited in the plasma wave is calculated to be only < 1.4 mJ. Hence, the total energy removed from the pump is <~1% of the pump energy available during the 7 ps interaction period, so the saturation is not due to pump depletion. The saturation of the power scattered from the pump beam is demonstrated to be only weakly dependent on time over the 3.5 ps period

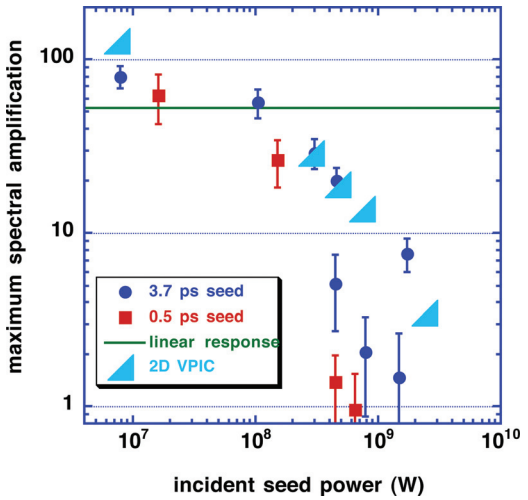

FIG. 5. (Color) The measured maximum spectral amplification factor vs. seed power for both 0.5 and 3.5 ps duration seeds is shown compared with predictions of the linear model and the 2D VPIC simulations, which demonstrates that the amplification rate at low power is well described by both linear and VPIC models and the saturation of the amplification at high power is also captured by VPIC as discussed in the text.

which we drive the scattering Langmuir wave by a second series of measurements with 0.5 ps duration seed pulses. The reduced duration seed produces similar amplification factors to the longer duration case when the seed power is low, and also demonstrates a reduction of the amplification factor as the seed power is increases to 4.5×10^8 W. These measurements identify the saturation mechanism as purely electron kinetic because the saturation occurs in a time that corresponds to only one inverse wave frequency ($t_{pulse} \sim w_{iaw}{}^{-1}$) for the ion acoustic waves that are produced by the secondary decay of the Langmuir wave on longer time scales.

III. COMPARISON OF RAMAN AMPLIFICATION EXPERIMENTS WITH VPIC SIMULATIONS

Using VPIC (Refs. 27, 28, and 32) kinetic plasma simulations with a binary collision model to treat inter-particle Coulomb collisions,[33] we have modeled the experiments in two spatial dimensions.[34] In the simulations, the spatial domain is 1 mm in the pump laser direction and 0.5 mm in the transverse direction and the plasma is initialized with a uniform density profile having density, plasma composition, and initial temperature consistent with the experiments. The pump is a flat-top, long pulse launched from the left of the simulation domain with an average intensity 1.02×10^{14} W/cm^2. The seed, launched from the right of the simulation domain, is Gaussian in time with 3.5 ps FWHM and has a central wavelength of 1200 nm; this pulse counter-propagates at 11° relative to the pump direction and is shown schematically in Figure 6. Both pump and seed intensity profiles have random distributions of speckles of sizes equal to the diffraction limited spot sizes; the correlation time of the speckles in the seed are set equal to twice the observed amplification spectral width to ensure all components with significant amplification are included.

SRS initiates in the simulations when the seed and pump interact in the plasma and the amplification factor is found to

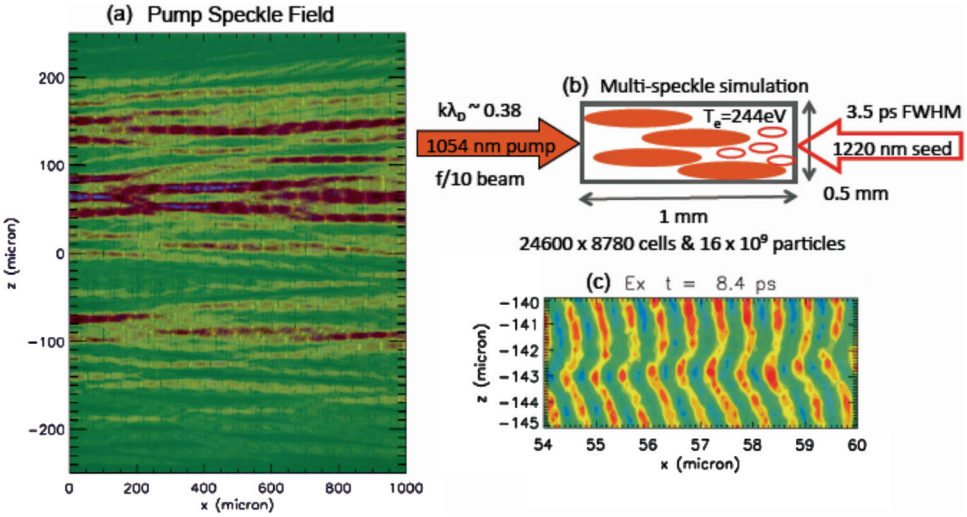

FIG. 6. (Color) (a) The VPIC simulations for the Jupiter experiments use a pump beam with a spatial profile of the intensity that includes realistic hot spots as shown. (b) The uniform plasma conditions for the simulations in (a) are shown along with the pump and seed beam parameters, with the seed 11° from counter propagating with the pump. (c) The simulated profile of the Langmuir wave amplitude shows marked bowing of the wave front at the highest seed power studied, consistent with electron trapping and electron kinetic saturation of Raman amplification in this case.

decrease as the seed intensity increases, as observed experimentally. The electron distribution in the simulations also develops a supra-thermal component in the direction of the Langmuir wave, consistent with electrons being trapped by the wave. Moreover, as shown in Figure 6, the simulations show evidence of nonlinear wave front bowing and electron plasma wave self-focusing,[28] as well as an associated reduction in the amplification factor at high intensity, as seen in the experimental observations, and find collisions significantly affect the observed amplification only at low seed energy.

The two primary results from the comparison of Jupiter experiments and the VPIC modeling of them are (1) the first observation of nonlinear saturation of scattering stimulated by a broad spectrum, short pulse seed undergoing Raman amplification with a small amplitude gain exponent and (2) quantitative agreement in amplification factor from experiments and first-principles, 2D VPIC simulations of the electron kinetic effects. These results provide computational tools that have been benchmarked in plasmas with dimensionless parameters similar to those in ignition targets (as shown in Table I) for a model of stimulated scattering by multiple intersecting beams that can be used to optimize laser coupling in ignition experiments. The model developed here includes primarily electron kinetic effects acting on ps time scales that are expected to modify the growth rate of the Langmuir waves responsible for Raman scattering, and can therefore play a substantial role in determining the overall scattering. This model does not, as yet, include larger spatial and time scale effects, such as filamentation, secondary ion wave decays, and hydrodynamic interactions considered in more detail in Ref. 45 and elsewhere, which may also influence the scattering.

IV. MEASUREMENTS AND MODELING OF MULTI-PUMP SBS AMPLIFICATION EXPERIMENTS WITH THE OMEGA LASER

In this section we discuss experiments that demonstrate that light amplified by more than one counter-propagating pump beam in an under-dense plasma produces total scatter that is enhanced above both the original seed of light and the light scattered by a single pump and seed combination. This validates a second important aspect of our multi-beam scattering models for NIC. The multi-pump amplification studied occurs with beam and plasma conditions similar to what are expected in ignition targets and is compared to the linear model of SBS scatter.

The experiments were carried out at the Omega laser facility[35] in plasmas produced by twenty eight 351-nm heater beams with a total energy of 4.2 kJ in a 1.5 ns, flat in time, pulse incident on a 3 micron thick CH foil target as shown in Figure 7 and described in Ref. 36. The heater beams are unsmoothed, pointed together at a point on the surface of the foil at its center. The heaters are focused 3.9 mm past the surface of the foil, so that the FWHM of the intensity profile transverse to the direction of propagation is 590 μm at the surface. The plasma conditions are simulated with the Hydra code[31] indicating the plasma density, temperature, and flow conditions at 1.4 ns are appropriate for resonant SBS amplification of a seed beam with the same wavelength as the pumps that cross near 330 microns above the surface of the foil. At these positions the plasma density is 4% of critical, the electron temperature is 1.4 keV, and the outward directed flow velocity is near Mach 1. A seed beam of 351 nm light is propagated down the axis of the foil plasma with its best

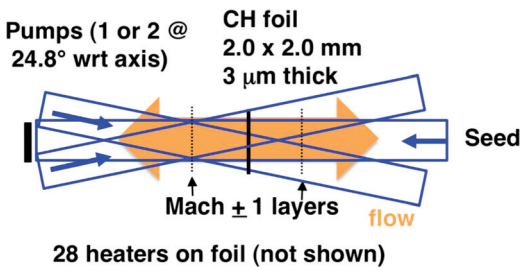

FIG. 7. (Color) The geometry of multi-pump SBS amplification experiments carried out at the Omega laser to demonstrate the cumulative effect of two pump beams on scattered light under plasma conditions similar to ignition. The experiments are performed with a pre-heated exploding foil target that produces the Mach 1 plasma flow layer needed to match the SBS resonance when both pump and seed have a 351 nm wavelength.

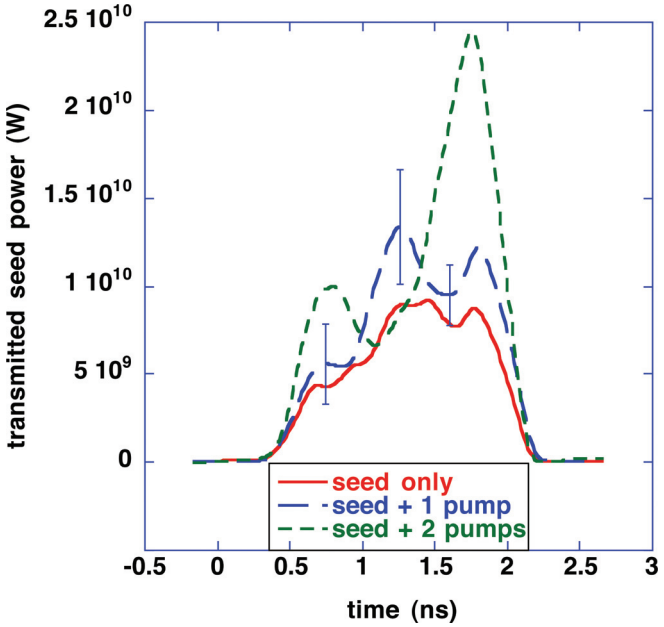

FIG. 8. (Color) The measured power transmitted though the plasma for the case of 1 and 2 crossing pump beams as well as no pump beams. The transmission is clearly enhanced or amplified, in the vicinity of the 1.4 ns time corresponding to the time when the simulations indicate the SBS amplification resonance is centered in the beam crossing volume. The amplification of the 2 pump case relative to the no pump case is clearly larger than that of the 1 pump case relative to no pumps, as expected from the multi-beam scattering model.

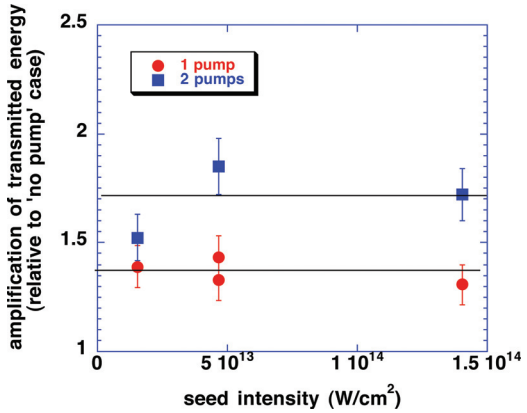

FIG. 9. (Color) The time integrated, or energy, amplification factor measured in a series of experiments with different seed intensities, and with both 1 and 2 pump beams, showing the 2 pump amplification is larger than the 1 pump value in all cases studied and that the amplification values are only weakly dependent on the seed intensity as expected by the linear model of SBS amplification.

focus placed beyond the foil to produce a spot diameter of 165 microns FWHM in the interaction region. The incident energies are 4.2, 16, and 458 J and the pulse is 1.5 ns long. The f/6.6 seed beam is delayed 0.5 ns with respect to the heater beams. The transmission of the seed beam in the absence of pumps is measured by a detector collecting the entire f/cone of the incident beam as discussed in Ref. 36 and shown in Figure 8.

The seed beam is observed to be resonantly amplified in experiments with both one and two crossing, pump beams. In these experiments each pump beam is incident with 375 J of 351 ns light in a 1.5 ns flat pulse, at a 23° angle from counter-propagating with the seed. In addition each pump beam is smoothed with a distributed phase plate (DPP) that produces a best focus spot of 165 microns FWHM at the point where the beams cross the seed beam axis. The effect of the SBS resonance on the seed power is determined by comparison of the transmitted seed power in an experiment with no pumps to that in experiments with one and two pumps (Figure 8). The transmission with a 15 J seed is measured in the "one pump" case and is observed to be increased. The increase is especially clear near 1.4 ns when the effect is expected to be maximum as discussed in Ref. 36. This incident seed energy was repeated with each of the two identical pump beams in the one pump configuration and the average of the two measurements is shown as the one pump waveform in Figure 8 with the difference in the two measurements represented by the error bars shown. The observed variability in the transmitted seed power case may be due to hydrodynamic variation in the plasma flow from shot to shot, which would cause the resonance location to move in the interaction volume. Next, a second pump beam was introduced, crossing the seed at the same point as the first and with the same energy, pulse shape, and timing. The most important result is that the transmitted seed power in the "two pump" case has a maximum much greater than either the "one pump" or "no pump" cases, clearly demonstrating that the total induced scatter is increasing as the number of crossing pump beams is increased. In fact the ratio of the peak power in the "two pump" case to the "no pump" power at the same time gives a peak amplification by a factor of 2.9 with two pumps, whereas the same comparison for the "one pump" case shows a peak amplification factor of 1.6. For comparison the gain exponent calculated from our multibeam interaction model, when assuming the ion wave response is linear and the plasma profiles are those simulated in 2D is $=0.87$ for a single pump with a uniform intensity profile propagating in a straight line though the plasma. The $0.6\times$ reduction of the exponent in the experiment likely due to the 3D nature of the resonance layer and beam crossing volume as well as possibly limited non-linear wave saturation effects. It is also note worthy that in this case the effect on the amplification of adding a second crossing pump beam at an angle to drive a different ion wave is very similar to what would be expected if the energy of the second pump was added to the first pump, consistent with expectation of linear models. Further experiments demonstrate that the observed amplification is a response to the ponderomotive force of the pump and seed, and not due to hydrodynamic effects such as heating by the pump, by demonstrating the dependence of the amplification on the relative polarization of the pump and probe beam. These additional experimental results are described in Ref. 36.

The dependence of the observed amplification on the number of pump beams and on the intensity of the seed beam was studied in a series of experiments with zero, one, and two pump beams. We show consistency between these experiments by integrating over the pulse shown in Figure 8 and considering the time integrated energy amplification factor as shown in Figures 9 and 10. Figure 9 shows that the

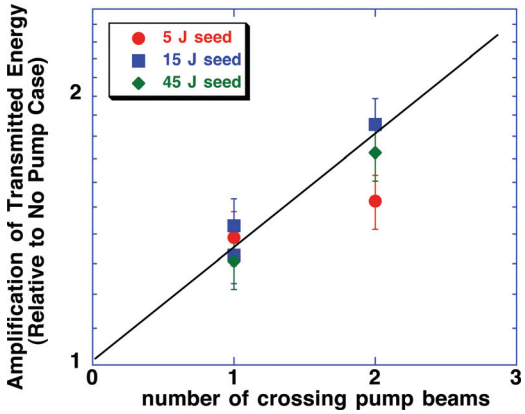

FIG. 10. (Color) The energy amplification factors from Figure 9 plotted vs. the number of pump beams, also showing the amplification factor increases in all cases studied, and further that in most cases it is close to the exponential scaling with number of pump beams predicted by the linear model of SBS amplification.

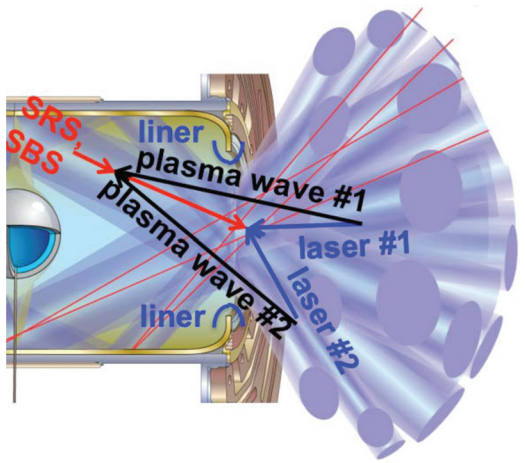

FIG. 11. (Color) Diagram of the geometry of one side of the symmetric hohlraum targets used for ignition experiments showing 96 beams grouped in 24 quads entering the laser entrance hole (LEH) at for different angles with respect to the axis (23.5°, 30°, 44.5°, and 50°), and the location of the liner material on the LEH. The geometry of the coupled three wave processes of the multi-beam interactions in the beam crossing volume, and the potential seeds of single beam SRS and SBS scattering coming from the hohlraum interior are also shown schematically.

transmitted energy is amplified in all cases where pump beams are present and the energy amplification factor exhibits a weak dependence on seed energy as is expected for a linear response of the ion acoustic waves to the ponderomotive force of the beams. In addition we observed the energy amplification factor to increase nearly exponentially with the number of pump beams as also expected for a linear wave response and shown as a line in Figure 10. These data demonstrate that both scattered power and energy increase as the number of resonant crossing pump beams is increased, consistent with the model of stimulated scattering from multiple laser beams we are now employing for ignition target designs.[37] The amplification with both one and two pumps observed in this case is consistent with a linear wave response and the two pump effect results from the addition of the gain exponents observed with each individual pump beam.

V. APPLICATION OF THE MULTI-PUMP AMPLIFICATION MODELS TO OBSERVATIONS OF SCATTER IN NIC TARGETS

Having benchmarked a linear model of SBS and SRS amplification as well as a simulation that can capture the non-linearity of SRS in cases where it was observed, the analysis of designs for targets for NIC was carried out in a two step process. First, the hydrodynamic simulations of the target were performed to indicate the expected plasma and beam conditions (as, for example, in Ref. 15), and estimates were made of the wavelengths and magnitudes of the scattering produced by the individual quads of beams.[8] Next, the region in which the quads intersect was analyzed to determine the amplification factors the light would experience as it left the target with the specified plasma conditions, and with the range of wavelengths and propagation directions of the scatter from individual beams in the interior. The gain exponents for backscatter from individual quads originating in the interior of the hohlraum are calculated using the LIP post-processor.[8] We assume that the backscatter light backtracks the path of the incident light in each quad, and calculate the coupling of the backscattered light as it exits the hohlraum to each of the incoming intersecting quads via a separate Langmuir wave for each pump as shown schematically in Figure 11. The coupling uses a linear kinetic model and is estimated in the 1D limit but for a full 3D geometry,[37] in a very similar way to the model described in Ref. 16. The coupling is calculated for one individual backscatter wavelength at a time. For a given backscatter seed of light, each intersection with an incoming quad will create a plasma wave which will lead to amplification of the seed by the laser pump. The effect of each quad is typically small but its accumulation with successive quads can lead to significant amplification of the seed. An early result of this effort was to identify the potentially deleterious effects of increased plasma density in the beam crossing volume near the laser entrance hole. Prior to the first NIC experiments the advantage of reducing the diameter of the laser electron hole (LEH) to minimize the loss of x-ray power from the hohlraum was recognized. This advantageous effect of small LEHs is traded off against the increased accumulation of ablated material from the edge of the holes in the region where the beams propagate. When the edge of the LEH is the same high Z material as the rest of the hohlraum wall, the increased plasma density accumulating in the beam crossing volume creates unacceptable absorption of beams before reaching the point where power deposition is desired in the interior near the hohlraum walls. The absorption problem could largely be overcome, however, by putting a thin CH coating on the lip of the laser entrance hole, as shown in Figure 11 which then resulted in a significant density of low Z plasma accumulating in the beam crossing region. These considerations led to the design of NIC targets with reduced size LEHs lined with CH, as well as a series of experiments with a much smaller version of the CH lined, reduced LEH diameter, target at the Omega laser facility. The tests at

OMEGA (Ref. 38) showed that the lined targets had increased stimulated Raman scattering associated with suprathermal electron generation and reduced x-ray drive, which was attributed to single beam effects in the modified plasma profile that the liner produced, and, though recognized as a potential source of ignition capsule preheat, the experimental findings were not considered enough of a concern to change the plan for the LEH lined targets in NIC. NIC hohlraums with reduced diameter, lined, LEHs were subsequently analyzed by the multi-beam model prior to the commencement of NIC experiments with the plasma and beam profiles taken from the best plasma models available and using the linear wave model for both SRS and SBS amplification in the crossing volume. The results showed that for the designs considered both the SBS and SRS re-amplification gain produced by all of the 23 crossing quads was increased relative to designs with large un-lined LEHs that were otherwise similar. The effect was especially pronounced for the inner cone of beams (defined as the cones of beams entering the hohlraum at angles of 23.5° and 30° with respect to the axis), for which the single beam SRS from the interior was expected to be the largest, and the reamplification exponents were several or larger. Subsequent analysis of smaller scale Omega hohlraum experiments indicated that the multibeam interaction is much reduced at small scale primarily due to reduced interaction lengths, and as a result the Omega tests are expected to under-estimate the multi-beam effects for NIC. These findings directed the designs for the majority of ignition and ignition emulator targets to the more conservative, large LEH approach, and led to a dedicated experiment to test the effect of the small, lined LEHs on scatter and x-ray drive in NIC scale targets. Figure 12 shows the SRS re-amplification vs. wavelength calculated with the linear model for all the entering beams in a scale 0.9 ignition emulator design driven with a shaped pulse (described in more detail in Ref. 39) both with small (56% of hohlraum diameter) CH lined LEHs, and with larger (64%) un-lined LEHs. Note that with the target with the liner, the plasma density in the beam crossing region increased the scatter not only because of increases in the peak SRS reamplification gain exponent, but also due to shifts of the peak closer to the wavelengths generated by scatter by the individual beams in the interior. The combination of these effects was predicted to produce sufficient multi-beam amplification and scatter in ignition designs that the hohlraum coupling efficiency would be significantly degraded.

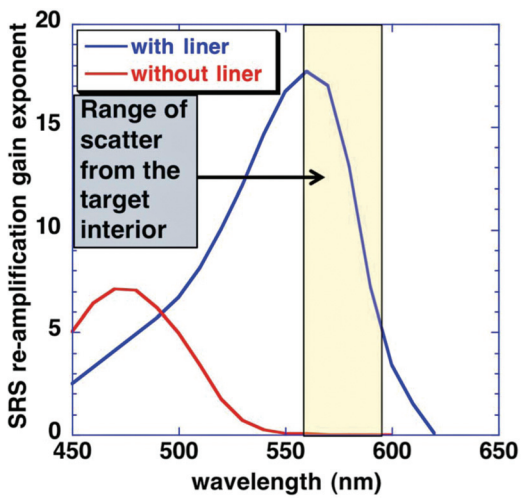

FIG. 12. (Color) The cumulative amplification exponent for SRS leaving scale 0.9 ignition emulator targets is calculated for both a large, un-lined LEH hohlraum and a reduced size, CH lined LEH hohlraum, showing that not only is the peak Raman amplification increased by the lined LEH, but the wavelength of the maximum effect is shifted close to the range of wavelengths expected by scattering from the interior, both of which cause the lined LEH target to have larger scatter and reduced coupling.

Both a single lined and multiple un-lined LEH scales 0.9 hohlraums were studied in the initial experiments for NIC. The scattering on a quad of beams incident at 30° with respect to the axis was measured with the Full Aperature Backscatter Station (FABS) and Near Backscatter Imager (NBI) diagnostics.[40,41] The thermal x-ray drive observed through the laser entrance hole was measured with the Dante diagnostic,[42] while the higher energy x-rays were measured with the Filtered fluorescer Experiment (FFLEX) diagnostic[43] and used to determine changes in the hot electron population. The time resolved spectrum of SRS scattering is shown in Figure 13, along with a spectral line out taken when the pulse is at peak power (t = 9.5 ns). In addition to measurements that show that the total SRS energy reflectivity from the four beams in the 30° quad that is diagnosed is increased by 1.9×, with scattered energy rising from 1665 J ± 20% (with 10950 J ± 20% incident with 3.91 Terawatt (TW) in the shaped pulse[39]) in the case with no liner, to 3352 J ± 20% (with 11600 J ± 20% incident with 4.15 TW peak in the shaped pulse) in the case with the liner. The incident powers reported for this beam do not account for the transfer of forward energy between inner and outer cones which is expected to be minimal in the un-lined hohlraum, and based on modeling is expected to increase the inner cone energy by 1.45 × in the case with the liner. Perhaps the most important observation in this experiment is also apparent in Figure 13 where the SRS scatter produced when the incident pulse reaches peak power at 9.5 ns was shifted to shorter wavelengths by the reduced size of the LEH and the CH liner consistent with the SRS emanating from lower density regions where the beams cross. The spectrally resolved power indicates that individual spectral components of the power at this time have enhancements that are still larger than the overall energy enhancement. It is clear that the greatest increase in SRS in the lined, small LEH target is observed at wavelengths shorter than the peak value for the un-lined, large LEH target, which is where the model indicates re-amplification is most active, although the wavelengths of peak SRS are shifted somewhat from the predictions in Figure 12, presumably due to small differences in the simulated and actual plasma conditions. The spectra shown in Figure 13 show changes in the scatter produced by the modifications to the LEH region, but the ratio of the two measurements cannot be directly compared to the calculated re-amplification factors shown in Figure 12 because simulations indicate that the changes in the LEH also modify the plasma profiles somewhat in the hohlraum interior so that the spectrum of scatter produced by the individual beams in

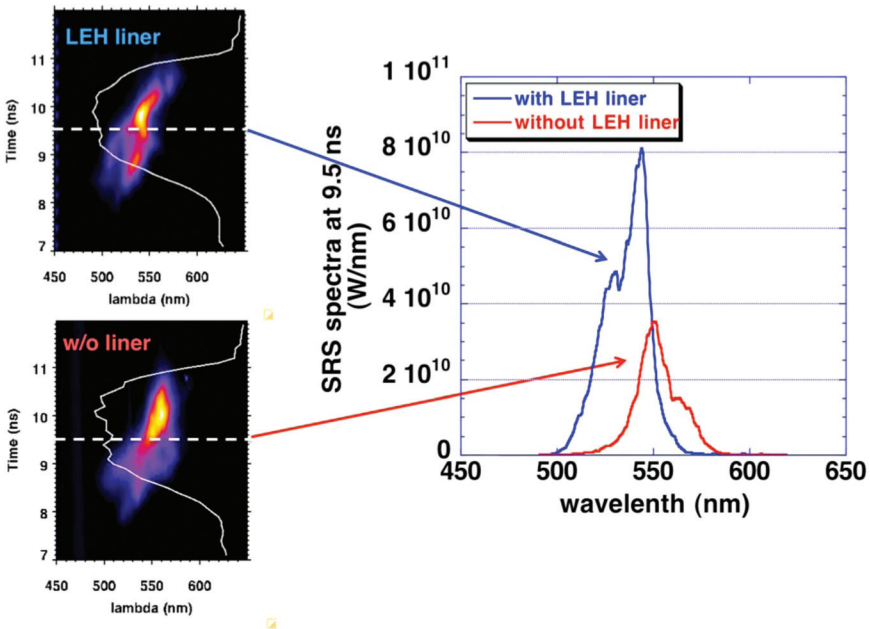

FIG. 13. (Color) Time resolved measurements of the SRS spectrum produced by the two targets analyzed in Figure 12, show that total SRS scattering is increased by 1.9× in the case of the lined LEH, and that the short wave length scatter shows the greatest increase, as discussed in the text.

the interior that seed the multi-beam effects in the crossing beam region is not expected to be the same in these two cases. In particular, the greatest enhancement in the scattered spectrum is observed at still shorter wavelength than the calculations in Figure 12 would suggest. Further the x-ray power, as measured by Dante, showed a reduction of 0.57 (± 0.05) × for the lined target compared to the un-lined (with total incident energies being very similar; 510 kJ vs. 485 kJ, respectively) which when compared with the increase in scatter on the 30° beams accounting for about 14% of the incident energy, suggests that even greater scattering occurred on the un-diagnosed 23° beams or in other directions to cause the observed reduction in x-ray drive. Hence, the Dante measurements were also consistent with the expectation that the lined target would produce increased total scatter that would offset the reduced x-ray loss rate and produce a reduction in the overall level of x-ray drive achieved in the hohlraum. Finally, the hot electron spectra, as measured by the FFLEX diagnostic of the emitted x-ray spectra, were determined to be well fit by a Gaussian with 10 ± 3 kJ of energy and a temperature of 18.5 keV in the case with the liner and with 5.0 ± 1.5 kJ of energy and a temperature of 29 keV, in the case with no liner, which is also consistent with SRS being more energetic in the low density region of the target, when the liner is present[43] qualitatively consistent with expectations. While quantitative calculations of SRS in these targets is still under development these measurements are qualitatively consistent with the predictions of the linear model of multi-beam scattering and confirmed the selection of the large, un-lined, LEH ignition target for NIC based on that model.

The remainder of the NIC experiments carried out to date have further verified the needed hohlraum conditions for the ignition campaign are produced in the targets with un-lined LEHs as described in Ref. 39 culminating in studies with scale 1.07 targets with 1.0–1.3 MJ of energy incident. As a result of the many measurements made in these experiments the models of plasma formation have been revised and now give much closer agreement with all measurements as described in Ref. 44. Analysis of the scattered SRS spectrum as well as predictions from the linear multi-beam scattering model using the revised plasma profile information, allows the role multibeam effects on the SRS to be assessed in the scale 1.07 ignition target. The scattered spectrum measured in the quad of 30° beams in the 470–620 nm range for the case of 1.01 MJ of incident energy is shown in Figure 14. The total scattered energy detected on this quad was 5181 J (with 26700 J incident, with 6.8 TW peak in the shaped pulse[39]). The time dependent wavelength of the peak scatter,

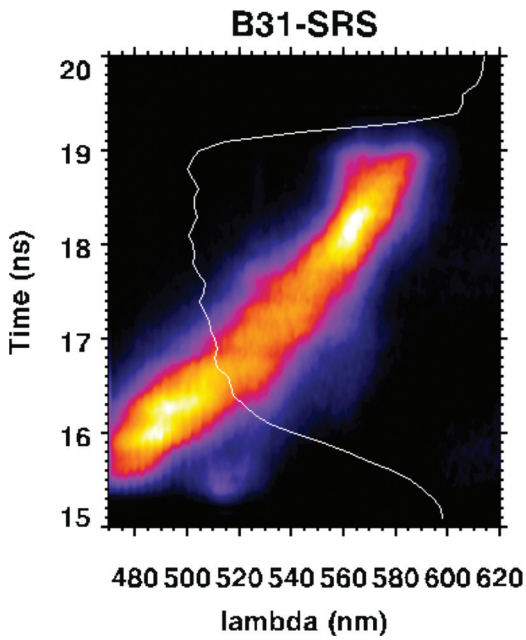

FIG. 14. (Color) Time resolved measurements of the SRS spectrum produced by the 1 MJ scale 0.9 ignition target showing shorter wavelengths at early time, and with the time of the spectral measurement of Figure 15 indicated.

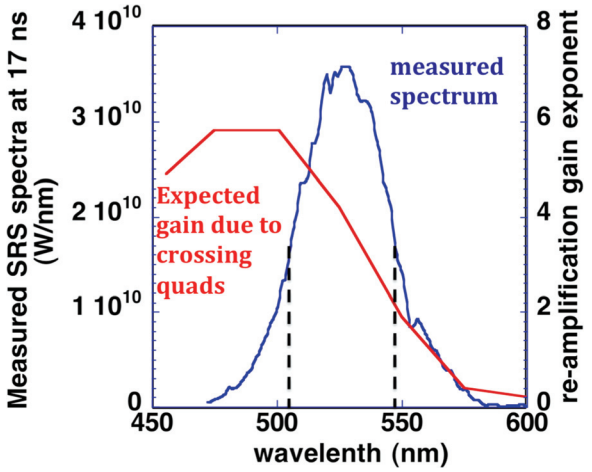

FIG. 15. (Color) The SRS amplification exponents predicted for the 1 MJ, scale 0.9 target using the simulated plasma profiles and beam conditions at 17 ns compared with the measured spectrum of SRS from that target, showing that the SRS light observed would experience amplification by a factor of exp (2 to 5.8) depending on wavelength, as it transits the beam crossing region if the waves are linear. This indicates that multi-beam scatter can be a substantial component of the total scatter for these targets.

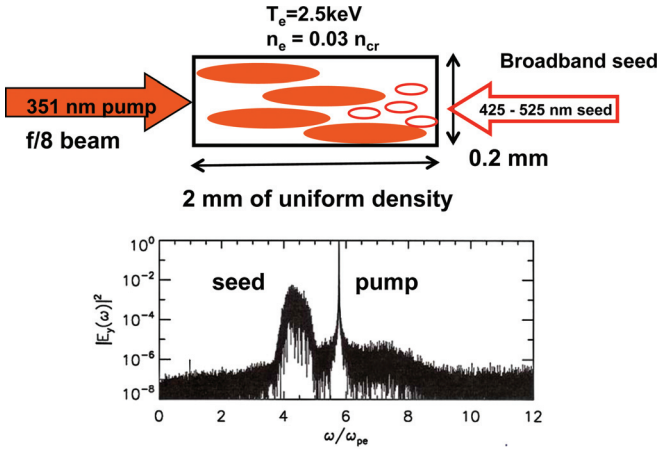

FIG. 16. (Color) Geometry and conditions for VPIC simulation of SRS amplification in the 1 MJ, Scale 0.9 target plasma conditions at 17 ns, uses a uniform plasma profile, a 200 micron slice of the 1.1 mm wide beams, and a single counter-propagating pump to simplify computations and verify the wave response and scattering for this case. The amplified probe spectrum is also shown as discussed in the text.

as well as the levels of scatter late in time, which are shown in Figure 14 have been shown to be in agreement with the LIP code and with extensive simulations with PF3D only when the effects of the two nearest crossing beams are included as described in Ref. 45. This study was motivated, in part, by the predictions of the linear model, which indicate the two nearest neighbor beams have the highest gain exponents, and its conclusions are further verification of the model. In addition the LIP analysis suggested that the total SRS gain exponent at the wavelength of peak scatter at 17 ns would be only 75% of the peak value at 18.6 ns when only the two nearest neighbor beams were included, indicating that SRS power at early time should be much lower than late time if there were no interaction with the remaining beams. However the observations in Figure 14 show that the early time SRS is comparable to or slightly brighter than that at late time, suggesting additional beams may be producing further amplification. In fact, our linear model of the gain exponents produced by all the crossing beams, based on the new plasma model parameters, predicts gain exponents in the range of 2–5.8 for the range of wavelengths observed at 17 ns as shown in Figure 15, while those produced by nearest neighbor beams alone are in the range of <2. This indicates that the additional beams are sufficient to significantly enhance the early time SRS and make it more comparable to the observations, provided the wave response is close to the linear values. Moreover these gain exponents also make it clear that a linear response of the waves in the beam crossing volume would make most of the scattered power observed at 17 ns due to the crossing beams.

To determine the effects of electron kinetic saturation that could limit the multibeam scatter in this case, we have done an initial simulation approximating the early time conditions in the NIC target using the 2D VPIC simulations that are benchmarked with the Jupiter experimental data of Figure 5. These simulations model a 200 micron wide by 2 mm long section in center of the 30° quad of beams in the region where they intersect the majority of the beams near the LEH and where their diameter is 1.1 mm. The region is filled with a uniform plasma with a density and temperature chosen to match the part of the simulated plasma profile where the linear models predict high gain from the crossing quads ($n/n_{crit.} = 0.03$, $T_e = 2.5$ keV). The seed of SRS from the interior of the target is then modeled as a Gaussian spectrum peaked at 475nm with a full width of 100 nm (i.e., 425 to 525 nm). The seed has a spatial profile that is a sum of random intensity variations that have a width appropriate to a diffraction limited spot produced by an f/8 quad of beams. The amplitude of each spot is randomly generated using an exponential distribution of intensities. To produce the desired spectrum, each region in the intensity profile is given a new, random amplitude and phase at the rate needed to produce the desired spectral width. The fields are smoothly interpolated in time between these values. The pump beam is counter-propagating with the seed (with the crossing angle neglected to minimize computation demands in this case) and has a spatially averaged intensity representing a single polarization component in two crossing quads of beams from the experiments (2.9×10^{14} W/cm^2), with its spatial intensity profile also determined from a random exponential distribution of appropriately sized regions and independent of time. The intensity of the seed is set to be 1.3×10^{13} W/cm^2 in this initial case, and the spectrum of light at the output of the interaction volume is amplified with a sharpened and shifted peak at $\omega/\omega_p \sim 4.3$ as shown in Figure 16. The simulation shows the interaction with the two pump beams results in up to 20% of the pump power leaving the interaction region as backscatter, and shows an overall amplification factors of 3.2× to 4× in the first several ps of interaction as shown in Figure 17. In addition a simulation done in the same geometry and conditions as the VPIC simulation using PF3D (Ref. 45) determined the linear response of the waves, and showed a peak spectral amplification factor of 4.2× demonstrating that the electron kinetic wave saturation effects that were observed in the Jupiter experiments, and

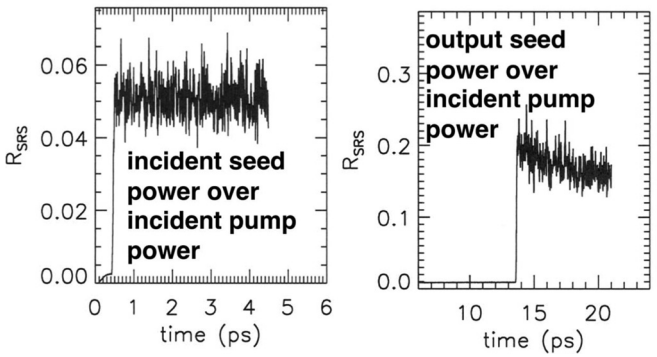

FIG. 17. The incident and transmitted SRS power waveforms from the VPIC simulations indicate an overall amplification of 3× to 4× similar to predictions of the linear wave model prediction for this case. This confirms that wave non-linearity is weak in the early time LEH plasma where $k\lambda_D$ is higher than in the Jupiter experiments, and allows multi-beam SRS scatter to be significant in this case.

captured by the VPIC simulation, do not make a large correction to the power scattered by a linear model of the waves in the case of a two crossing pump beam propagating in a plasma with conditions relevant to the early time of the 1 MJ, scale 1.07 NIC target. As a result of this analysis of the early time period and the analysis of nearest neighbor beams at late time,[45] it is clear that the effect of multiple crossing beams on the backscatter is substantial in this target as was initially predicted by the linear model.

VI. SUMMARY AND CONCLUSIONS

The effects of multiple intersecting laser beams in ignition targets have been analyzed by a suite of simulations that are benchmarked by small scale experimental measurements and have provided guidance and understanding for the results obtained in the initial ignition experiments. A linear model of the ion and electron wave response to the multiple crossing beams in the region of the laser entrance hole as well as light scattered from the interior of the target has successfully guided the design of ignition hohlraums to minimize the plasma density in the beam crossing volume. Experiments with the Jupiter laser have confirmed a linear response of the Langmuir waves producing SRS amplification at low scattered power and demonstrated an electron kinetic saturation at higher scattered power. Experiments at the Omega laser facility have show that when amplification by crossing beams occurs the total scatter scales up with the number of crossing pumps, under conditions similar to what is expected in ignition targets. These results have benchmarked the linear wave response model used to analyze the ignition targets, and the VPIC simulations that are being used to analyze aspects of the ignition experiments for which saturation may be important. The combined results of these experimentally benchmarked simulations have been used to improve the design of the ignition targets by indicating the advantages of larger laser entrance holes without low Z liners and to demonstrate that the effects of the multiple crossing beams are responsible for a significant fraction of the scattered SRS power at early time in the ignition targets studied experimentally so far, as well as to provide tools for studying SRS saturation in these targets.

[1]J. D. Lindl, P. Amendt, R. L. Berger, S. G. Glendinning, S. H. Glenzer, S. W. Haan, R. L. Kauffman, O. L. Landen, and L. J. Suter, Phys. Plasmas **11**, 339 (2004).
[2]W. L. Kruer, *The Physics of Laser Plasma Interactions* (Addison-Wesley, Redwood City, California, 1988).
[3]B. J. MacGowan, B. B. Afeyan, C. A. Back, R. L. Berger, G. Bonnaud, M. Casanova, B. I. Cohen, D. E. Desenne, D. F. BuBois, A. G. Dulier, K. G. Estabrook, J. C. Fernandez, S. H. Glenzer, D. E. Hinkel, T. B. Kaiser, D. H. Kalantar, R. L. Kauffman, R. K. Kirkwood, W. L. Kruer, A. B. Langdon, B. F. Lasinski, D. S. Montgomery, J. D. Moody, D. H. Munro, L. V. Powers, H. A. Rose, C. Rousseaux, R. E. Turner, B. H. Wilde, S. C. Wilks, and E. A. Williams, Phys. Plasmas **3**, 2029 (1996).
[4]D. S. Montgomery, B. B. Afeyan, J. A. Cobble, J. C. Fernández, M. D. Wilke, S. H. Glenzer, R. K. Kirkwood, B. J. MacGowan, J. D. Moody, E. L. Lindman, D. H. Munro, B. H. Wilde, H. A. Rose, D. F. Dubois, B. Bezzerides, and H. X. Vu, Phys. Plasmas **5**, 1973 (1998).
[5]R. K. Kirkwood, R. L. Berger, C. G. R. Geddes, J. D. Moody, B. J. MacGowan, S. H. Glenzer, K. G. Estabrook, C. Decker, and O. L. Landen, Phys. Plasmas **10**, 2948 (2003).
[6]J. D. Moody, B. J. MacGowan, J. E. Rothenberg, R. L. Berger, L. Divol, S. H. Glenzer, R. K. Kirkwood, E. A. Williams, and P. E. Young, Phys. Rev. Lett. **86**, 2810 (2001).
[7]E. Moses, R. Boyd, B. Remington, C. Keane, and R. Al-Ayat, Phys. Plasmas **16**, 041006 (2009).
[8]D. E. Hinkel, D. A. Callahan, A. B. Langdon, S. H. Langer, C. H. Still, and E. A. Williams, Phys. Plasmas **15**, 056314 (2008), and reference therein.
[9]L. Divol, R. L. Berger, N. B. Meezan, D. H. Froula, S. Dixit, P. Michel, R. London, D. Strozzi, J. Ross, E. A. Williams, B. Still, L. J. Suter, and S. H. Glenzer, Phys. Plasmas **15**, 056313 (2008), and references therein.
[10]W. L. Kruer, S. C. Wilks, B. B. Afeyan, and R. K. Kirkwood, Phys. Plasmas **3**, 382 (1996).
[11]R. K. Kirkwood, B. B. Afeyan, W. L. Kruer, B. J. MacGowan, J. D. Moody, D. S. Montgomery, D. M. Pennington, T. L. Weiland, and S. C. Wilks, Phys. Rev. Lett. **76**, 2065 (1996).
[12]R. K. Kirkwood, D. S. Montgomery, B. B. Afeyan, J. D. Moody, B. J. MacGowan, C. Joshi, K. B. Wharton, S. H. Glenzer, E. A. Williams, P. E. Young, W. L. Kruer, K. G. Estabrook, and R. L. Berger, Phys. Rev. Lett. **83**, 2965 (1999).
[13]R. K. Kirkwood, B. J. MacGowan, D. S. Montgomery, B. B. Afeyan, W. L. Kruer, D. M. Pennington, S. C. Wilks, J. D. Moody, K. Wharton, C. A. Back, K. G. Estabrook, S. H. Glenzer, M. A. Blain, R. L. Berger, D. E. Hinkel, B. F. Lasinski, E. A. Williams, D. Munro, B. H. Wilde, and C. Rousseaux, Phys. Plasmas **4**, 1800 (1997).
[14]E. A. Williams, B. I. Cohen, L. Divol, M. R. Dorr, J. A. Hittinger, D. E. Hinkel, A. B. Langdon, R. K. Kirkwood, D. H. Froula, and S. H. Glenzer, Phys. Plasmas **11**, 231 (2004).
[15]P. Michel, L. Divol, E. A. Williams, S. Weber, C. A. Thomas, D. A. Callahan, S. W. Haan, J. D. Salmonson, S. Dixit, D. E. Hinkel, M. J. Edwards, B. J. MacGowan, J. D. Lindl, S. H. Glenzer, and L. J. Suter, Phys. Rev. Lett. **102**, 025004 (2009).
[16]P. Michel, S. H. Glenzer, L. Divol, D. K. Bradley, D. Callahan, S. Dixit, S. Glenn, D. Hinkel, R. K. Kirkwood, J. L. Kline, W. L. Kruer, G. A. Kyrala, S. Le Pape, N. B. Meezan, R. Town, K. Widmann, E. A. Williams, B. J. MacGowan, J. Lindl, and L. J. Suter, Phys. Plasmas **17**, 056305 (2010); G. A. Kyrala, J. Kline, N. M. Hoffman, S. R. Goldman, S. Dixit, S. Glenzer, D. Kalantar, D. Bradley, N. Izumi, N. Meezan, O. Landen, D. Callahan, S. V. Weber, J. P. Holder, S. Glenn, M. J. Edwards, J. Koch, R. Prasad, R. Kirkwood, L. Suter, S. Haan, R. Town, B. Hammel, P. Michel, J. Milovich, T. Ma, R. Heeter, R. London, and J. Kilkenny, Phys. Plasmas **18**, 056307 (2011).
[17]H. X. Vu, D. F. DuBois, and B. Bezzerides, Phys. Rev. Lett. **86**, 4306 (2001).
[18]K. Y. Sanbonmatsu, H. X. Vu, B. Bezzerides, and D. F. Dubois, Phys. Plasmas **7**, 1723, (2000); K. Y. Sanbonmatsu, H. X. Vu, D. F. DuBois, and B. Bezzerides, Phys. Rev. Lett. **82**, 932 (1999).
[19]R. K. Kirkwood, B. J. MacGowan, D. S. Montgomery, B. B. Afeyan, W. L. Kruer, J. D. Moody, K. G. Estabrook, C. A. Back, S. H. Glenzer, M. A.

Blain, E. A. Williams, R. L. Berger, and B. F. Lasinski, Phys. Rev. Lett. **77**, 2706 (1996).
[20]J. C. Fernandez, J. A. Cobble, B. H. Failor, D. F. DuBois, D. S. Montgomery, H. A. Rose, H. X. Vu1, B. H. Wilde, M. D. Wilke, and R. E. Chrien, Phys. Rev. Lett. **77**, 2702 (1996).
[21]C. G. R. Geddes, R. K. Kirkwood, S. H. Glenzer, K. Estabrook, B. I. Cohen, P. E. Young, C. Joshi, and K. B. Wharton, Phys. Plasmas **10**, 3422 (2003).
[22]D. S. Montgomery, J. A. Cobble, J. C. Fernández, R. J. Focia, R. P. Johnson, N. Renard-LeGalloudec, H. A. Rose, and D. A. Russell, Phys. Plasmas **9**, 2311 (2002).
[23]J. L. Kline, D. S. Montgomery, L. Yin, D. F. DuBois, B. J. Albright, B. Bezzerides, J. A. Cobble, E. S. Dodd, D. F. DuBois, J. C. Fernández, R. P. Johnson, J. M. Kindel, H. A. Rose, H. X. Vu, and W. Daughton, Phys. Plasmas **13**, 055906 (2006).
[24]R. K. Kirkwood, E. Dewald, C. Niemann, N. Meezan, S. C. Wilks, D. W. Price, O. L. Landen, J. Wurtele, A. E. Charman, R. Lindberg, N. J. Fisch, V. M. Malkin, and E. O. Valeo, Phys. Plasmas **14**, 113109 (2007).
[25]Y. Ping, R. K. Kirkwood, T.-L. Wang, D. S. Clark, S. C. Wilks, N. Meezan, R. L. Berger, J. Wurtele, N. J. Fisch, V. M. Malkin, E. J. Valeo, S. F. Martins, and C. Joshi, Phys. Plasmas **16**, 123113 (2009).
[26]R. K. Kirkwood, Y. Ping, S. C. Wilks, N. Meezan, P. Michel, E. Williams, D. Clark, L. Suter, O. Landen, N. J. Fisch, E. Valeo, V. Malkin, D. Turnbull, S. Suckewer, J. Wurtele, T. L. Wang, S. F. Martins, C. Joshi, L. Yin, B. J. Albright, H. A. Rose, and K. J. Bowers, J. Plasma Phys. (2010).
[27]L. Yin, B. J. Albright, K. J. Bowers, W. Daughton, and H. A. Rose, Phys. Rev. Lett. **99**, 265004 (2007).
[28]L. Yin, B. J. Albright, K. J. Bowers, W. Daughton, and H. A. Rose, Phys. Plasmas **15**, 013109 (2008).
[29]V. M. Malkin and N. J. Fisch, Phys. Plasmas **12**, 044507 (2004).
[30]V. Malka, C. Coulaud, J. P. Geindre, V. Lopez, Z. Najmudin, D. Neely, and F. Amiranoff, Rev. Sci. Instrum. **71**, 2329 (2000); S. Semushin and V. Malka, *ibid*. **72**, 2961 (2001).
[31]M. M. Marinak, G. D. Kerbel, N. A. Gentile, O. Jones, D. Munro, S. Pollaine, T. R. Dittrich, and S. W. Haan, Phys. Plasmas **8**, 2275 (2001).
[32]K. J. Bowers, B. J. Albright, L. Yin, B. Bergen, and T. J. T. Kwan, Phys. Plasmas **15**, 055703 (2008); K. J. Bowers, B. J. Albright, B. Bergen, L. Yin, K. J. Barker, and D. J. Kerbyson, Proceedings of the ACM/IEEE Conference on Supercomputing, Austin, 2008 (IEEE, New York, 2008), pp. 1–11.
[33]T. Takizuka and H. Abe, J. Comput. Phys. **25**, 205 (1977).
[34]L. Yin *et al*., (unpublished).
[35]J. M. Soures, R. L. McCrory, C. P. Verdon, A. Babushkin, R. E. Bahr, T. R. Boehly, R. Boni, D. K. Bradley, D. L. Brown, R. S. Craxton, J. A. Delettrez, W. R. Donaldson, R. Epstein, P. A. Jaanimagi, S. D. Jacobs, K. Kearney, R. L. Keck, J. H. Kelly, T. J. Kessler, R. L. Kremens, J. P. Knauer, S. A. Kumpan, S. A. Letzring, D. J. Lonobile, S. J. Loucks, L. D. Lund, F. J. Marshall, P. W. McKenty, D. D. Meyerhofer, S. F. B. Morse, A. Okishev, S. Papernov, G. Pien, W. Seka, R. Short, M. J. Shoup, M. Skeldon, S. Skupsky, A. W. Schmid, D. J. Smith, S. Swales, M. Wittman, and B. Yaakobi, Phys. Plasmas **3**, 2108 (1996).
[36]R. Kirkwood *et al*., Phys. Rev. E (submitted).
[37]P. Michel *et al*., (unpublished).
[38]S. P. Regan, T. C. Sangster, D. D. Meyerhofer, W. Seka, R. L. McCrory, C. Stoeckl, V. Yu. Glebov, N. B. Meezan, L. J. Suter, D. J. Strozzi, E. A. Williams, W. L. Kruer, O. S. Jones, D. A. Callahan, M. D. Rosen, O. L. Landen, S. H. Glenzer, C. Souce, and B. J. Macgowan. Bull. Am. Phys. Soc. **53**, 89 (2008).
[39]N. B. Meezan, L. J. Atherton, D. A. Callahan, E. L. Dewald, S. Dixit, E. G. Dzenitis, M. J. Edwards, C. A. Haynam, D. E. Hinkel, O. S. Jones, O. Landen, R. A. London, P. A. Michel, J. D. Moody, J. L. Milovich, M. B. Schneider, C. A. Thomas, R. P. J. Town, A. L. Warrick, S. V. Weber, K. Widmann, S. H. Glenzer, L. J. Suter, B. J. MacGowan, J. L. Kline, G. A. Kyrala, and A. Nikroo, Phys. Plasmas **17**, 056304 (2010); S. H. Glenzer *et al*., Phys. Rev. Lett. **106**, 085004 (2011).
[40]A. Mackinnon, C. Niemann, K. Piston, G. Holtmeier, T. McCarville, G. Jones, I. Reinbachs, R. Costa, J. Celeste, R. Griffith, R. Kirkwood, B. MacGowan, and S. Glenzer, Rev. Sci. Instrum. **77**, 10E529 (2006), this reference describes an older version of the NBI diagnostic.
[41]R. K. Kirkwood, T. Mccarville, D. H. Froula, B. Young, D. Bower, N. Sewall, C. Niemann, M. Schneider, J. Moody, G. Gregori, F. Holdener, M. Chrisp, B. J. MacGowan, S. H. Glenzer, and D. S. Montgomery, Rev. Sci. Instrum. **75**, 4174 (2004), this reference describes an older version of the FABS diagnostic.
[42]E. L. Dewald, K. M. Campbell, R. E. Turner, J. P. Holder, O. L. Landen, S. H. Glenzer, R. L. Kauffman, L. J. Suter, M. Landon, M. Rhodes, and D. Lee, Rev. Sci. Instrum. **75**, 3759 (2004).
[43]J. McDonald, L. Suter, O. Landen, J. Foster, J. Celeste, J. Holder, E. Dewald, M. Schneider, D. Hinkel, R. Kauffman, L. Atherton, R. Bonanno, S. Dixit, D. Eder, C. Haynam, D. Kalantar, A. Koniges, F. Lee, B. MacGowan, K. Manes, D. Munro, J. Murray, M. Shaw, R. Stevenson, T. Parham, B. Van Wonterghem, R. Wallace, P. Wegner, P. Whitman, B. Young, B. Hammel, and E. Moses, Phys. Plasmas **13**, 032703 (2006).
[44]R. P. J. Town, M. D. Rosen, P. A. Michel, L. Divol, J. D. Moody, G. A. Kyrala, M. B. Schneider, J. L. Kline, C. A. Thomas, J. L. Milovich, D. A. Callahan, N. B. Meezan, R. E. Olson, D. E. Hinkel, E. A. Williams, R. L. Berger, M. J. Edwards, L. J. Suter, S. Dixit, S. H. Glenzer, O. L. Landen, H. A. Scott, J. A. Harte, and G. B. Zimmerman, Phys. Plasmas **18**, 056302 (2011).
[45]D. Hinkel M. D. Rosen, E. A. Williams, A. B. Langdon, C. H. Still, D. A. Callahan, J. D. Moody, P. A. Michel, R. P. J. Town, R. A. London, and S. H. Langer, Phys. Plasmas **18**, 056312 (2011).